Engineering Structures 33 (2011) 1450–1458

Contents lists available at ScienceDirect

Engineering Structures

journal homepage: www.elsevier.com/locate/engstruct

The effect of the infill in arched structures: Analytical and numerical modelling

António Sousa Gago *, Jorge Alfaiate, António Lamas

IST - Department of Civil Engineering and Architecture, Technical University of Lisbon, Portugal

ARTICLE INFO

Article history:
Received 26 October 2009
Received in revised form
15 December 2010
Accepted 29 December 2010
Available online 25 February 2011

Keywords:
Arch
Masonry
Bridge
Infill
Arch-infill interaction
Load carrying capacity

ABSTRACT

Although arches, vaults and domes were essential structural elements in ancient engineering works, their structural analysis presents a challenge to modern designers. It was well known by the medieval builders that infill is essential for the stability of arched structures. Nevertheless, some disasters occur nowadays due to incorrect infill removal, usually done with the purpose of decreasing the applied load. In the present work a comprehensive analysis of the infill influence on the structural behaviour of arched structures is performed. For this purpose analytical models based on equilibrium considerations and finite elements models are used. Experimental results obtained from the Bargower bridge destructive test, are used to calibrate the numerical results. Some conclusions regarding the structural behaviour of arched structures and modelling strategies are presented.

1. Introduction

Although spanning space has always been a big challenge in bridge and building design, few structural solutions are available to architects and engineers for large spans. Among them the suspension cable, the beam or truss, the arch and their 3D derivatives, vaults and domes are the most widely used [1]. The arched structural shape, invented 6000 years ago in Mesopotamia [2] and perfected by the Romans in the first millennium BC, was, until the Industrial Revolution, the system almost exclusively used for large spans.

The arch transmits the self-weight and the applied loads to the supports through compressive stresses, enabling the use of non-tensile strength materials, such as stone or brick masonry. Thus, by using such structural shapes, the master masons could disregard the lack of tensile strength of masonry, and take advantage of its high level of durability, compressive strength and incombustibility to build grand and lasting structures. Until then, the use of linear structural elements forced the adoption of either high tensile strength materials, such as wood (usually not very durable), or reduced spans.

Although arches, vaults and domes, were essential structural elements in ancient engineering works, their structural analysis presents a challenge to modern designers, trained in the scope of steel and reinforced concrete structures. This is due to two main reasons: (i) the traditional structural theory, developed under the assumptions of a linear elastic behaviour applied to a continuum, is not suitable to model discontinuous, non-tensile resistant masonry structures; and (ii) the modern concepts of structural design, based on strength, strain and stability analysis, are not applicable to arched masonry structures. For example, an arch submitted to concentrated increasing loads may fail while exhibiting insignificant stresses or strains [3], demonstrating that stress based analyses, defined in most building codes, are inadequate for masonry arches.

Safety of arched masonry structures, when suitably supported, depends upon the relation between shape, ring thickness and loading characteristics — namely the distribution and magnitude of the load [4]. Therefore, the design of arched masonry structures is a quest for the most suitable shape with respect to loading and boundary conditions. This geometrically based design approach, common in the past, remains relatively unknown to the present day designer. As a consequence, accidents may occur due to removal of the fill in the extrados of arches and domes, which are performed under the assumption of alleviating the loading when deformations occur (Fig. 1). In fact, although it was well known by the master masons that the infill is essential for the stability of the arched structures, the modern designers tend to ignore this knowledge.

It was at the end of the last century that the interest on masonry structures was revived. The most important contributions to the understanding of the structural behaviour of arches were made by Jacques Heyman [5–7], who also identified the importance of the fill in supporting vaults. After his pioneering work, other publications can be found in the literature [8–11], in which the

* Corresponding address: IST DECivil – Av. Rovisco Pais, 1049-001 Lisboa, Portugal. Tel.: +351 218418201 or +351 218418219; fax: +351 21 8418200.
E-mail address: gago@civil.ist.utl.pt (A.S. Gago).

0141-0296/$ – see front matter © 2011 Elsevier Ltd. All rights reserved.
doi:10.1016/j.engstruct.2010.12.037

Fig. 1. Damage in vaults due to the removal of the infill. Left: Bucelas Church (Lisbon, Portugal); right: Machico Church (Madeira, Portugal).

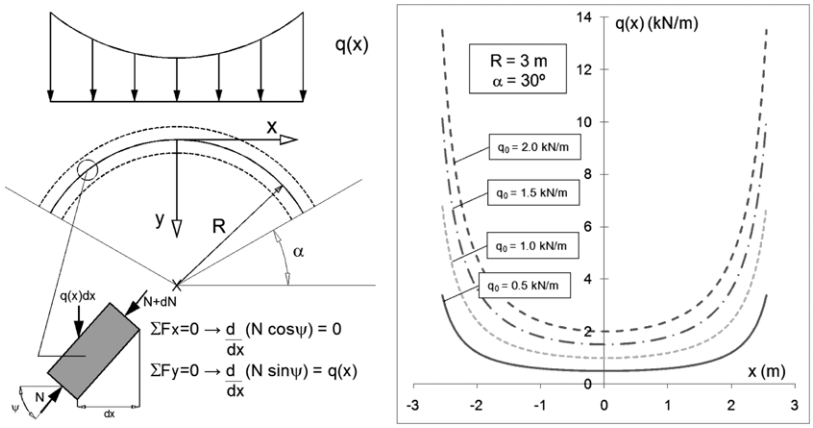

Fig. 2. Vertical loading corresponding to a circumferential line of thrust.

importance of the infill was detected, although this issue is not capital in those works.

Several computational modelling strategies have also been adopted to analyse masonry structures: some authors used physically non-linear finite elements with a discrete crack approach for the arch joints [12]; others used less detailed methods, for instance adopting a smeared crack approach [13,14], or making use of curved beam elements [15]. Finally, some authors also used different methods, such as the discrete element method [16,17].

The first aim of the present paper is to explain the favourable effect of the extrados infill in the stability of arched structures using modern structural analysis. A rational and not empirical interpretation of that effect may also contribute to the understanding of the behaviour of arches. Moreover, the paper describes the structural models developed for the study of arched structures and their calibration against experimental tests of the Bargower bridge conducted up to collapse.

The contributions in this paper consist of: (i) understanding the favourable influence of the infill on the structural behaviour of arches; and (ii) new modelling approaches, in which the effect of the infill is simulated with finite elements, both as an initial stress state, using a sequentially linear approach, and taking into account physically and geometrically non-linear effects. These approaches, were used to prove that the effects of the infill in the strength and stability of arches can be very important and must be considered in the repair of existing ones or in new situations.

2. The effect of the infill self-weight

The equilibrium of the arch cross-section implies that the stress resultant (thrust) is applied at an inner point [18–21]. The "line of thrust" is the locus of the application points of the stress resultant at each cross-section, i.e., it is the theoretical line that represents the path of the resultants of the compressive forces through the stone structure [22]. The stability of the arch can be estimated in relation to the line of thrust [23]: the arch is stable if it is possible to find at least one line of thrust lying inside the arch ring. Moreover, the closer this line is to the arch's axis, the higher the safety level.

Although empirically established since Leonardo da Vinci, this criterion for evaluating the stability of the arch based on the location of the line of thrust was only theoretically demonstrated in the second half of the twentieth century. Heyman's study of masonry structures using the Theory of Plasticity, in particular the Static and Kinematic Theorems, was a decisive contribution to the demonstration [5,24]. The application of the Theory of Limit Analysis to masonry elements is based on the hypotheses of (i) non-tensile strength, (ii) infinite compressive strength and (iii) sliding failure cannot occur. These hypotheses are valid for old stone masonry structures, even if the infinite compressive strength assumption is sometimes debatable.

Even though the arch is a statically indeterminate structure; a one-to-one correspondence between the (geometric) shape of the line of thrust and the loading can be obtained through equilibrium considerations. From the equilibrium of an infinitesimal portion of a circular arch of radius R for which the line of thrust coincides with the axis of the arch (Fig. 2), the corresponding vertical loading is given by the expression:

$$q(x) = \frac{q_0.R^3}{(R^2 - x^2)^{\frac{3}{2}}} \tag{2.1}$$

in which q_0 is a parameter defining the family of possible loadings.

Fig. 2 presents the loading profiles derived from Eq. (2.1). They correspond to smaller amplitude of loading at the crown

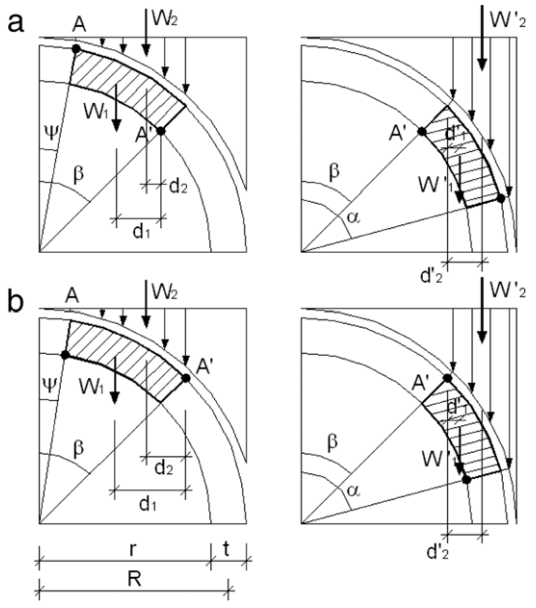

Fig. 3. Minimum admissible thickness of an arch loaded by its self-weight and by the self-weight of the infill. Limit situations of the line of thrust: (a) hinge at crown extrados; (b) hinge at crown intrados.

of the arch and larger amplitude near the abutments. Although the exact solutions provided by Eq. (2.1) are not admissible for semi-circular arches at $x = R$, it can be concluded that loads with similar profiles produce quasi circumferential lines of thrust and thus maximum safety levels in circular arches. The profile of the self-weight of an infill is a good approximation of these load patterns, thus explaining that the infill is beneficial for the structural stability of circular arches, which are most commonly adopted in old constructions.

As stated by Heyman [3,25], the minimum admissible thickness of a loaded arch is a measure of its structural stability, and the ratio between the arch's thickness and its minimum admissible value can be used to define a geometric safety coefficient. In this way, the favourable effect of the infill may be confirmed by evaluating the minimum admissible thickness of arches loaded under both their self-weight and the self-weight of the infill. If a decrease in the minimum admissible thickness is found when the infill's self-weight is considered, then the beneficial effect of the infill's self-weight is confirmed.

To evaluate the minimum thickness of the circular arch loaded by its self-weight and the self-weight of the infill, two limit situations must be considered, each corresponding to a different geometry of the line of thrust (Fig. 3): one where the self-weight of the arch (γ) is predominant (Situation 1 — external hinge at the crown); and the other where the self-weight of the infill (μ) has a major influence (Situation 2 — internal hinge at the crown). Following Ochsendorf's approach [21], the equilibrium analysis obtained from the work balance in each limit situation leads to two different relationships between the arch's minimum thickness and the ratio "arch self-weight – infill self-weight". In Fig. 4 the corresponding curves and envelope are shown, in which the ratio between the arch's self-weight (γ) and the infill's self-weight (μ) is represented in the x axis by $\mu[1 + (r/t)]/\gamma$ (r and R are the internal and mean radius of the arch, respectively). In this figure it can be seen that the infill contributes to the decrease of the minimum admissible thickness of the circular arch, with the corresponding increase in safety.

Beyond the favourable effect of the infill in bringing the line of thrust closer to the axis of the circular arch, it produces two additional important benefits: (i) the decrease of the ratio between the horizontal and vertical components of the thrust transmitted

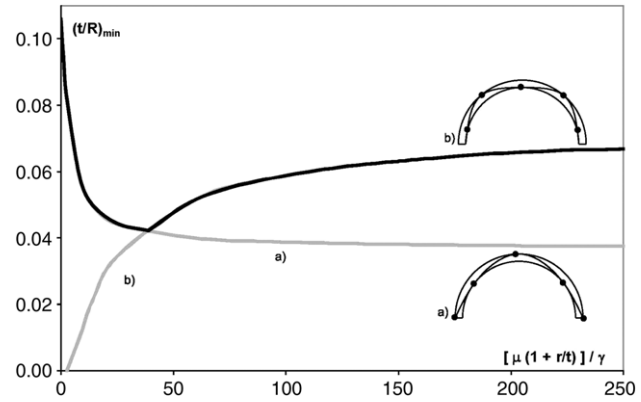

Fig. 4. Minimum admissible thickness (t) of a circular arch loaded by its self weight and by the self weight of the infill. Curves (a) and (b) correspond to (a) and (b) situations in Fig. 3.

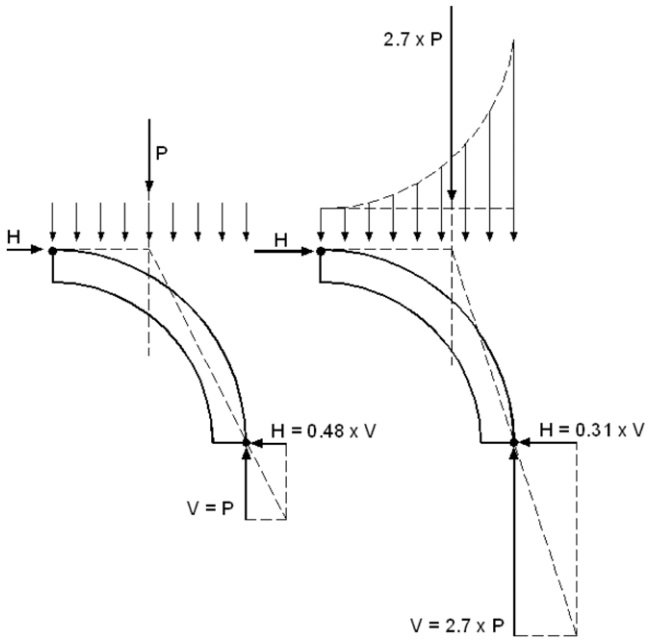

Fig. 5. Decrease of the ratio between the horizontal and vertical components of the thrust transmitted by the arch to the abutments.

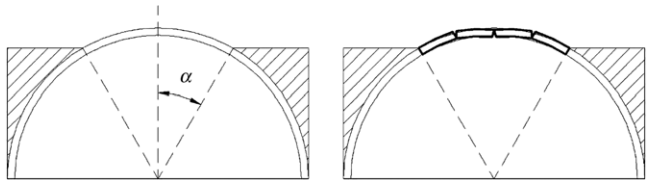

Fig. 6. Decrease of the effective span of the arch due to the restriction of the lateral movement of the loaded voussoirs.

by the arch to the abutments (Fig. 5) and (ii) the increase of the compressive stresses between the arch voussoirs. The former is a consequence of the resultant of vertical loads being closer to the abutment and may be taken as a measure of its stability. The latter gives rise to an increase of friction and decreasing risk of slippage between the arch voussoirs.

3. Other favourable effects of the infill

Apart from these favourable effects of the self weight of the infill, the presence of the infill material on the extrados of the

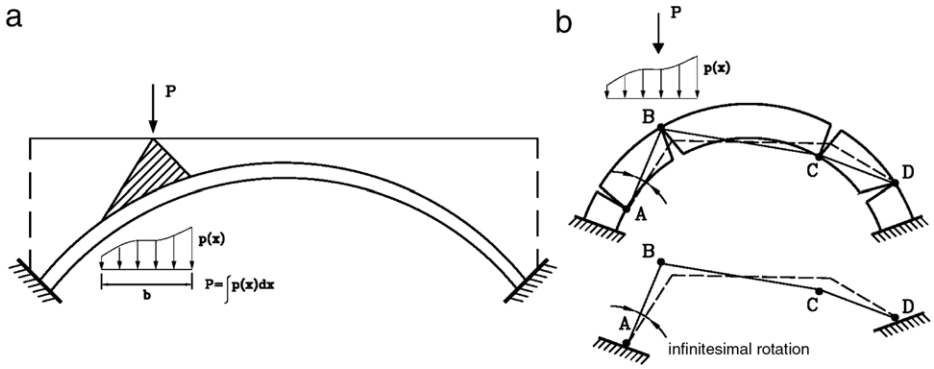

Fig. 7. (a) Schematic representation of the dispersion of loads along the infill, (b) 4 hinged mechanism and corresponding infinitesimal virtual displacements used to evaluate the collapse load.

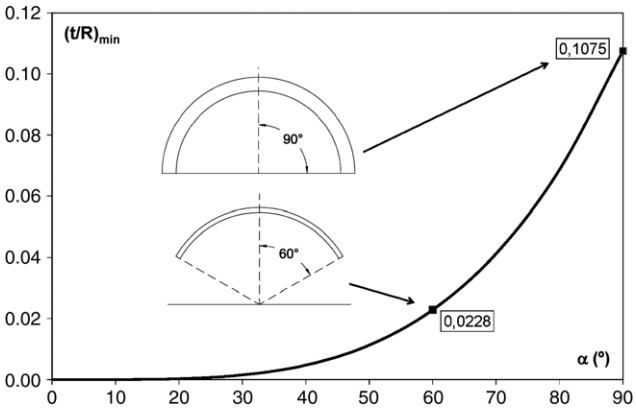

Fig. 8. Minimum admissible thickness of arches as a function of the cut off angle (α) (obtained following Ochsendorf's approach [21]).

arch induces other beneficial effects, such as: (i) a restriction of the lateral movement of the loaded voussoirs, giving rise to a smaller effective span of the arched structure (Fig. 6), and (ii) a distribution over a wider length of the arch of any load applied to the top of the infill (in-depth dispersion of the load, schematically represented in Fig. 7(a)), smoothing out, in particular, the effects of concentrated loads. In fact, if the infill presents sufficient stiffness to prevent horizontal movement of the arched structure, no hinges can form under the infill (Fig. 6). This allows for the line of thrust in the infilled region to be located outside the arch. In this case, a decrease of the effective span of the arched structure is obtained with a corresponding increase in stability, since a decrease of the opening angle gives rise to a significant decrease of the minimum admissible thickness (see Fig. 8). This fact was well known by the medieval builders, who often only filled the extrados of vaults at locations where it was needed to stabilize the structure (Fig. 9 [26]).

The advantageous effect of the in-depth dispersion of the loading can be evaluated using the mechanism method in the scope of the Limit Analysis Theory. As shown in Fig. 7(b), for the same admissible collapse mechanism, the spread load $p(x)$ gives rise to a smaller amount of work than the corresponding concentrated load P. Due to the energy balance in the mechanism method, a smaller work corresponds to a higher collapse load, and thus to a higher level of structure stability (further information on this mechanism method applied to masonry structures can be found in [27–29]).

4. Modelling the influence of the infill on the behaviour of arched structures

In the previous sections a simple analysis was performed on the effects of the self weight of the infill on the arch's behaviour. The

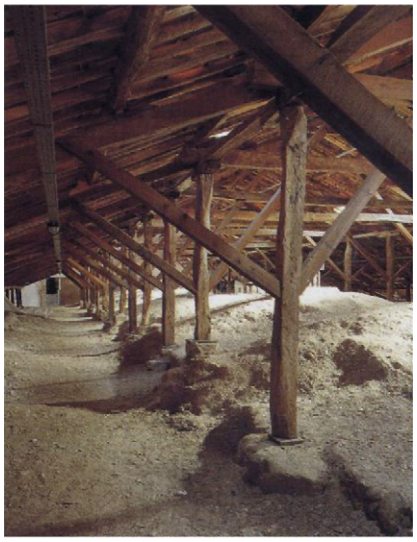

Fig. 9. Partially filled extrados of the vault of the central aisle of the XIVth century church of the Monastery of Alcobaça (Portugal) [26].

simplest way to model the influence of the infill in the extrados of arched structures is through the consideration of: (i) the vertical loading, due to its self weight and (ii) the horizontal loading, corresponding to the horizontal resistance forces from the infill material. However, to simulate the advantageous effects of the lateral stiffening due the infill on the arch extrados, more sophisticated models must be adopted namely finite element models and non-linear incremental analyses [30,31].

The authors have studied the Bargower bridge (destructive) experimental tests which provided data to verify the accuracy of these models [32,33], and to draw conclusions about the advantageous effects of the infill on the stability of arched structures. In the modelling of the arch of the Bargower bridge two different finite element models were used to simulate the infill: (1) the infill was simulated by an initial state of stress and by lateral springs; and (2), in a more sophisticated approach, the infill is explicitly modelled in the finite element mesh.

4.1. Description of the bridge and load test arrangement

The Bargower bridge arch ring had a semi-circular profile, built up of regular, cut to shape, sandstone voussoirs. The presence of one metre thick inner side walls made up of rubble masonry was detected behind spandrel dressed stone facing walls. Also, as discovered upon bridge demolition, arch haunching consisted of crushed sandstone with clay traces, above which spandrel filling

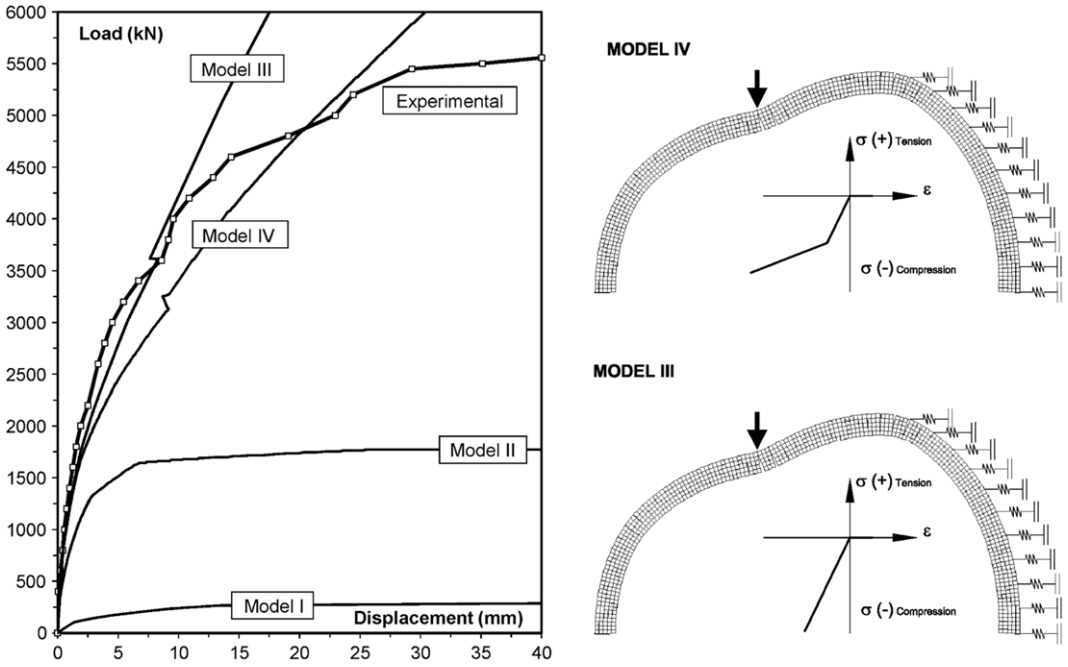

Fig. 10. Simplified finite element models: vertical displacement of arch soffit beneath load line.

Table 1
Bargower bridge principal dimensions.

Span	10.00 m
Rise at midspan	5.18 m
Arch thickness	0.588 m
Total width	8.68 m
Fill depth at crown	1.20 m

was constructed with a silty gravelly sand. The main dimensions are listed in Table 1.

Before the tests, the bridge was in a moderate conservation state, only demonstrating small defects that were found to have no significant influence on the overall structural capacity. Experimental tests on sandstone specimens revealed a compressive strength of 33.3 MPa and a Young's modulus of 14.1 GPa. The evaluated stone dead weight was 26.8 kN/m^3 and, from available data, the self weight of the infill was considered to be 20.0 kN/m^3. The test procedure consisted of the incremental application of load, by means of hydraulic jacks, to a concrete beam cast in the road surface across the full width of the bridge and located at one third of the span, where the minimum failure load was expected. The reactions of the jack against steel beams were supplied by ground anchors. For the purpose of this paper, attention should be focused on the vertical displacements measured at the load location and at the crown of the arch.

4.2. Numerical simulation — a simplified finite element model

In the less sophisticated approach, the masonry arch was modelled by continuum finite elements and the infill by an initial state of stress and by lateral spring supports (Fig. 10).

The joints were idealized as zero-thickness interface elements and the regularly shaped stone voussoirs were represented by continuum linear-elastic elements. Fracture, modelled by means of a discrete crack approach, was allowed only at the masonry joints by means of a tension free model. Penalty functions were introduced in the constitutive relations in order to prevent overlapping under crack closure. The material parameters used for the interfaces are given in Table 2. For the linear elastic continuum elements the experimental Young's modulus was used.

Table 2
Interface element properties.

Joint normal stiffness	10^{12} kN/m^3
Joint tangential stiffness	10^{12} kN/m^3
Tensile strength of joint	0

The infill contribution is modelled as a boundary condition, introducing horizontal spring supports at the extrados of the arch. These springs behave under compression only, according to either linear or bilinear elastic constitutive laws. The horizontal sub grade coefficient was assumed to vary linearly along the depth of the arch, between 0 and 3 MN/m^3, which is a good estimate for the material used in the bridge [34]. The initial state of stress was modelled by applying nodal loads equivalent to the self weight of both stone voussoirs and the infill and to the lateral earth pressure, which was assumed to be due to the initial steady-state ($k_0 = 0.45$). Test loading was simulated by means of nodal forces at the extrados of the arch ring, reproducing an approximate elastic dispersion of a transverse line load applied at the surface of the bridge deck. The contribution of the spandrel walls was ignored and absolute rigidity of the abutments assumed. Geometric non-linear effects were not included in the analysis.

It should be noted that according to the test description, the external spandrel walls (internal ones were not identified in the bridge), stiffer than the remaining arch, detached from it at an initial loading phase. As a consequence, the influence of the spandrel walls on the response of arch bridges [35] was disregarded in this section, namely in the numerical evaluation of the ultimate load. In the next section, the influence of the spandrel walls is analysed more in detail.

In this simplified model a non-iterative technique was introduced, based on a sequentially linear approach [36], in which changes in the stiffness are allowed only at the mortar joints and infill springs and the evaluation of the structural response was thus not incrementally obtained. Instead, the stiffness of the structure was reduced according to a material law, and equilibrium points on the structural response obtained by sequentially linear analyses.

Furthermore, no special algorithm for stiffness degradation (such as those defined in [36]) was necessary, since the tensile

free material adopted in the joints produces an abrupt extinction of the normal elastic stiffness. Non-proportional loading was considered with the sequentially linear approach, similar to the works presented in [37,38].

Four simulations were carried out using this finite element model. In Model I, the isolated arch was analysed considering the infill contribution limited to the vertical (self weight) loads. The obtained ultimate load value (about 300 kN) was far below the experimental one (circa 5600 kN), indicating that the effect of the horizontal restraint of the infill is relevant. Note, however, that the analysed arch has a thickness to radius ratio of $t/R = 0.102$, smaller than the minimum value required for the equilibrium of an isolated arch ($(t/R)\,\min = 0.1075$ — Fig. 8). The increase of strength obtained in Model I (from zero to 300 kN) is due to the effect of the infill self weight.

In Model II, the infill contribution was taken into account through the initial state of stress (both vertical and horizontal). The relationship between the line load and the deflection calculated beneath, in the vertical direction, is presented in Fig. 10. That relationship clearly presents a less stiff overall behaviour than the experimental curve and an ultimate load (circa 1700 kN) far below the maximum experimental value. It must be pointed out that with Model II the ultimate load increased by a factor of 6 when compared to the ultimate load obtained with Model I.

The big difference found between experimental results and numerical results from Model II indicates that the stiffness of the infill cannot be ignored, i.e., the effect of initial stress state, although important, must be complemented with the explicit modelling of the lateral stiffness introduced by the infill. Therefore, in the third simulation, designated by Model III, the interaction between the infill and the arch ring was attempted through both: (i) the initial state of stress and (ii) the restraint provided by linear elastic springs. As a consequence, the difference between numerical and experimental results improves considerably, showing the decisive contribution of arch haunching on bridge behaviour. However, the global structural stiffness does not decrease significantly at a later stage of the deformation process, giving rise to load values higher than the ultimate experimental load (see Fig. 10). In the fourth simulation (Model IV), a bilinear law was adopted for the springs, enabling, under increasing stress, a degradation of the stiffness to half the initial value and consequently a better approximation of the experimental data. In the curves obtained with Models II and IV a sudden recovery of the secant stiffness is found (with corresponding meaningless recovery of displacements), which is due to the non-incremental approach adopted.

From these numerical results it can be concluded that modelling of the infill effects is essential to predict the correct collapse load of arches, namely by taking into account: (i) the initial stress state, (ii) the lateral stiffening effect, and (iii) the infill stiffness degradation with increasing stress.

However, in both models III and IV, the ultimate experimental load was significantly overestimated and the stiffness degradation was not sufficiently decreased. This was due to the fact that the lateral stiffening effect was simulated by the simplified behaviour of springs with unbounded strength. This effect is better approximated in the next section, in which a more sophisticated description of the lateral confinement of the soil is adopted.

4.3. Numerical simulation — a more sophisticated finite element model

Due to the limitations of the simplified approaches described in 4.2 a more sophisticated model, with better characterization of the behaviour of the infill material, was developed.

As previously assumed, fracture was modelled by a discrete approach. It was allowed at the arch masonry joints and at the stone blocks-soil boundary by means of tension free and near-cohesionless frictional interfaces, respectively. The blocks were assumed to behave as linear-elastic and for the filling soil both linear elastic and Mohr Coulomb plasticity models were used. The joints between voussoirs were discretized using interface elements under mode-I fracture, using a zero tensile strength Rankine criterion. Upon crack opening, both zero shear traction and zero shear stiffness are assumed.

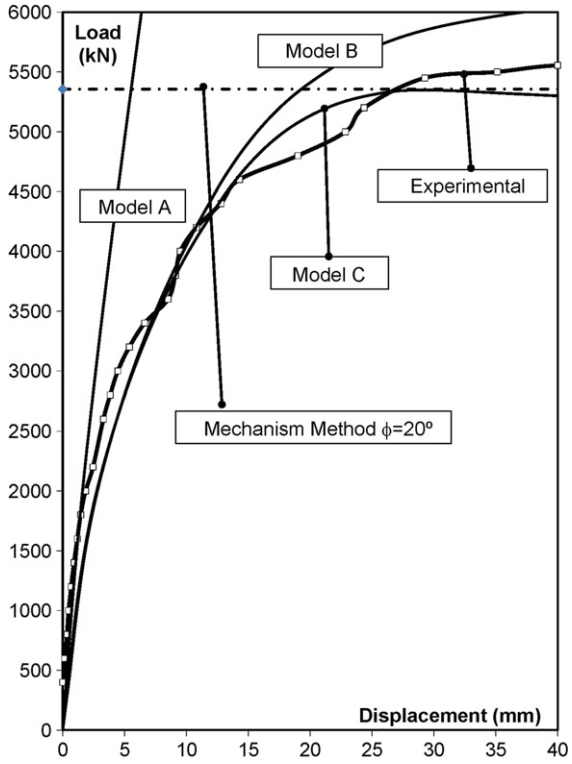

Fig. 11. A more refined finite element model: vertical displacement of the arch soffit beneath the load line.

The joints between the arch and the filling soil behave according to an associated plasticity friction model using a Mohr Coulomb yield criterion and a near zero cohesion value. The infill and the stone blocks were treated as two-dimensional elements. Although, at an initial stage of the experimental test, the external spandrel walls detached from the structure, they remained in a self equilibrium state. Thus, it is admissible to assume that enough lateral bearing capacity was left to sustain the infill. As a consequence, a plane strain state of the infill is assumed, induced by the lateral restraint of the spandrel walls. This hypothesis was also adopted in the works presented in [13,15]. The stone blocks were modelled using linear-elastic elements with a Young's modulus of 14.1 GPa. The filling was modelled as a near-cohesionless frictional material obeying the Mohr–Coulomb yield criterion with an associated flow rule. Regarding the boundary conditions of the infill, only the horizontal displacements are prevented at the vertical boundaries and both horizontal and vertical displacements are prevented at the bottom horizontal boundary (Fig. 15). A Young's modulus of 40 MPa and a friction angle of 30° were adopted for the infill as good estimations of the soil properties. The road surface was also modelled using a Mohr Coulomb plasticity model, in which free horizontal displacements at the lateral boundaries are adopted. The material parameters used for the interfaces and for the continuum elements given in Table 3 were either obtained experimentally or from parametric tests performed with the purpose of fitting the experimental results. As previously, overlapping at crack closure was prevented using a penalty formulation. In the voussoir joints

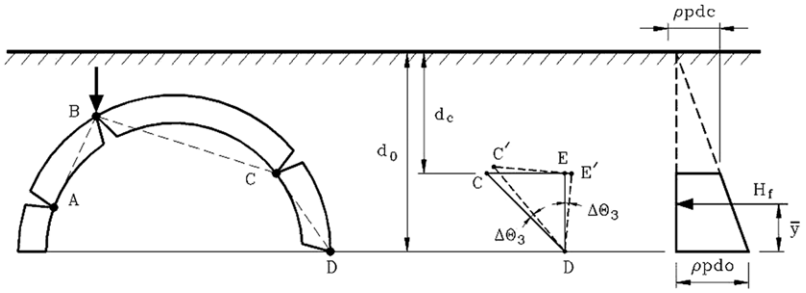

Fig. 12. Mechanism model: contribution of passive pressure.

Table 3
Finite element properties.

Joints	Between voussoirs	Between arch and soil
Normal stiffness (kN/m^3)	0.233×10^{11}	0.233×10^{11}
Tangential stiffness (kN/m^3)	0.104×10^{11}	0.104×10^{4}
Tensile strength (MPa)	0	–
Cohesion (MPa)	–	1×10^{-3}
Friction angle	–	20°
Dilatancy angle	–	20°
Continuum elements	Fill	Surfacing
E (MPa)	40	5×10^{3}
Cohesion (MPa)	1×10^{-3}	1.443
Friction angle	30°	30°
Dilatancy angle	30°	30°

a large value of the tangential stiffness was also used, since it is known that slipping does not play an important role in the collapse of arches [3].

The explicit contribution of the spandrel walls on both the stiffness and arch resistance was also ignored. The use of non-linear stress–strain relationships requires an incremental iterative procedure, i.e., the loads were applied step-by-step and equilibrium iterations were carried out at each increment until equilibrium is reached within acceptable limits. The arc-length method proved to be very useful for situations where the standard Newton–Raphson method fails, such as in the case of snap-back behaviour that is known to occur frequently in masonry structures [39]. In the tests presented, a monotonic increase of the main crack mouth opening displacement (CMOD) is enforced.

Several simulations were undertaken with this finite element model. In Fig. 11, the most relevant relations of the load-vertical deflection under the load line are presented.

A linear-elastic behaviour of the infill (Model A) was first assumed. Although in the first part of the test a good approximation between the numerical and the experimental stiffness of the structure was obtained, the decrease of the experimental stiffness observed at a later stage, could not be reproduced with the numerical model. It was evident that, in order to better approximate the collapse load, a non-linear behaviour should be adopted for the fill soil elements. A second model in which the infill elements obey the Mohr–Coulomb yield criterion was then adopted. With this model, both geometrically linear (Model B) and non-linear (Model C) analyses were performed. A very good approximation was obtained, especially in the case of the geometric non-linear analysis (Model C). In the latter case, the calculated ultimate load was very close to the experimental one, whereas in the former case, a higher value of the ultimate load was found. This shows that neglecting the geometric non-linear effects leads to a non-conservative estimation of the ultimate load. This difference is more pronounced as the arch span increases. For the dimensions of the Bargower bridge and for the stiffness assumed for the stone blocks and fill soil, the geometric linear model leads to an overestimation of 17% in the ultimate load. Taking into account the deformation level registered under the load, *circa* 25 mm, a considerable dependence on the geometrically non-linear effects is found. Such dependence, also obtained by Lourenço in [40] for displacements about 8 mm in circular arches with a diameter equal to 5 m, is a consequence of the relation between the arch geometry and the equilibrium conditions (such that the line of thrust remains within the thickness of the arch).

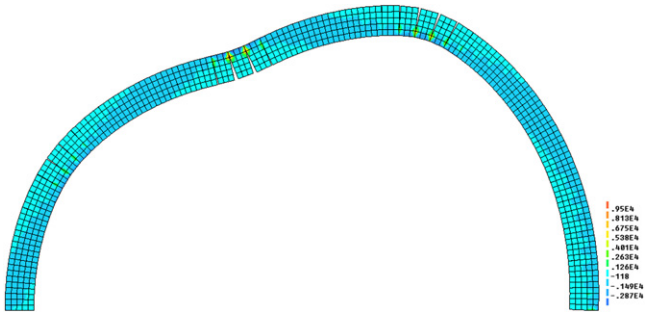

Fig. 13. Model C: principal stresses in the arch σ_I (kN/m^2).

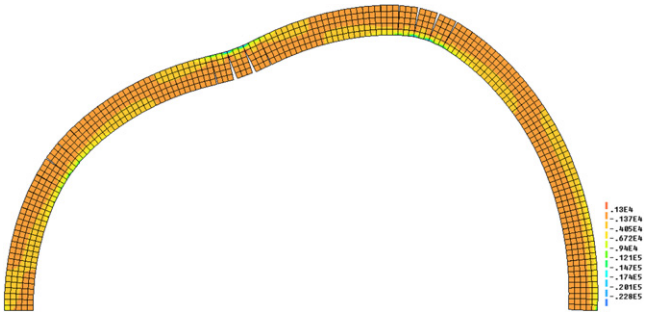

Fig. 14. Model C: principal stresses in the arch σ_{II} (kN/m^2).

In Fig. 11, the value of the collapse load obtained with the mechanism method [27] is also marked. With this method, in which small displacements were adopted, the contribution of the infill was taken into account considering the passive pressures of the soil acting only between the two hinges C and D at the right side of the arch (Fig. 12). Three different friction angles were used, 20°, 25° and 30°, corresponding to collapse loads of 5356 kN, 6299 kN and 7445 kN, respectively. Only the first case is shown in Fig. 11, but the use of the 20° value is questionable. In fact, adopting a friction angle of 30°, which leads to the best approximation using Model C, the mechanism method would predict an ultimate load much higher than the experimental ultimate load. This is due to the simplifications adopted in the mechanism method, in which the geometrically non-linear effects are also neglected. In fact, although the mechanism method provides useful benchmarks for the numerical analysis, the results of this method must be considered with caution.

In Figs. 13–18 the numerical results – namely principal stresses, plastic strains and deformed mesh – obtained for the ultimate

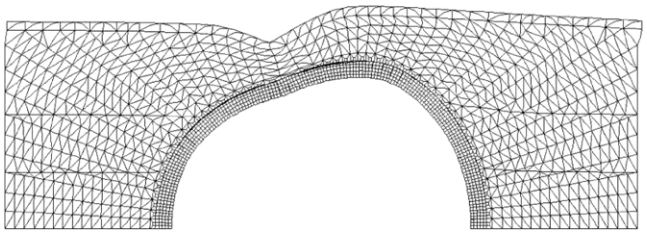

Fig. 15. Model C: deformed mesh for the ultimate load.

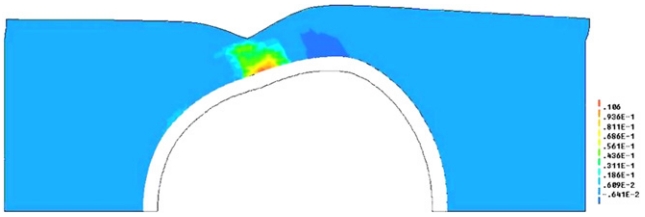

Fig. 16. Model C: plastic deformations ε_{xx} of the infill.

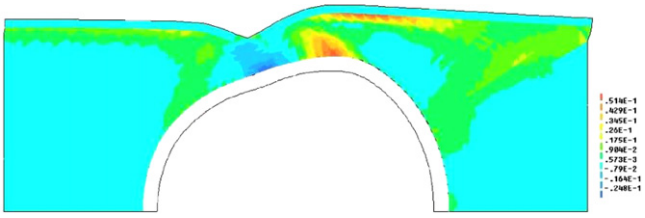

Fig. 17. Model C: plastic deformations ε_{yy} of the infill.

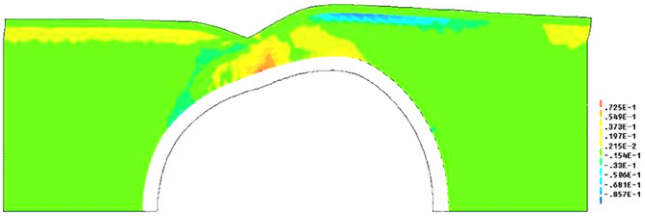

Fig. 18. Model C: plastic deformations ε_{xy} of the infill.

load in the Model C (with geometrically non-linear effects), are presented. Under the ultimate load, the maximum compressive stresses in the arch elements remain below the compressive limit of 33.3 MPa (Figs. 13 and 14). This validates the initial assumption of linear elastic behaviour of the blocks. In Figs. 16–18 the plastic strains of the infill are also presented, corresponding to the expected yielding pattern of the soil.

5. Conclusions

The present study demonstrates the importance of the extrados infill on the structural behaviour of arched structures. This is often neglected or misjudged by modern engineers who, in general, do not have a sufficient background in the design of these types of structures.

It was first shown that distributed loads similar in shape to the self-weight of the infill correspond to a circumferential line of thrust and, thus have a beneficial effect on circular arches since the safety level and stability of the structure increases and, accordingly, the minimum admissible thickness of the arch decreases.

It was subsequently shown that the self-weight of the infill also induces: (i) the increase of the relation between the vertical and the horizontal components of the thrust transmitted by the arch to the abutments, with corresponding increase of stability and (ii) the increase of the compressive stresses between voussoirs of arched structures. As a result, the overthrow of the abutments and the slipping of the voussoirs are less likely to occur, with a decrease of the corresponding risk of collapse.

Experimental results obtained from a destructive test on the Bargower bridge were used to calibrate the numerical models. They explain that the influence of the infill is not limited to its self-weight. In fact, the lateral pressure and stiffening due to the infill has a crucial influence on both the arch strength and stability.

This is why the infill must be explicitly taken into account in structural modelling and safety assessment. To evaluate the influence of the infill in arched structures, the corresponding lateral stiffening must be simulated by means of non-linear models such as those presented in the paper. The use of less accurate modelling methods is not recommended.

References

[1] Fitchen J. The construction of Gothic Cathedrals — a study of medieval vault erection. Chicago: The University of Chicago Press; 1981.
[2] Huerta S. Galileo was wrong: the geometrical design of masonry arches. Nexus Netw J 2006;8(2):25–6.
[3] Heyman J. The masonry arch. Ellis Horwood: Chichester; 1982.
[4] O'Dwyer D. Funicular analysis of masonry vaults. Comput Struct 1999;73: 187–97.
[5] Heyman J. The safety of masonry arches. Int J Mech Sci 1969;11:363–85.
[6] Heyman J. On the rubber vaults of the middle ages, and other matters. Gaz Beaux-Arts 1968;71(March):177–88.
[7] Heyman J. The estimation of the strength of masonry arches. Proc Inst Civ Engrs 1980;69:921.
[8] Cavicchi A, Gambarotta L. Collapse analysis of masonry bridges taking into account arch-fill interaction. Eng Struct 2005;27(4):605–15.
[9] Melbourne C, Wang J, Tomor A. A new masonry arch bridge assessment strategy (SMART). Bridge Eng J 2007;160–162:81–7.
[10] Orbán Z. UIC project on assessment, inspection and maintenance of masonry arch railway bridges. In: Proceedings of the 5th international conference on arch bridges ARCH'07. 2007. p. 3–12.
[11] Orbán Z, Gutermann M. Assessment of masonry arch railway bridges using non-destructive in-situ testing methods. Eng Struct 2009;31(10):2287–98.
[12] Betti M, Drosopoulos GA, Stavroulakis GE. On the collapse analysis of single span masonry/stone arch bridges with fill interaction. In: Proceedings of the 5th international conference on arch bridges ARCH'07. 2007. p. 617–24.
[13] Wang J, Melbourne C. Finite element analyses of soil-structure interaction in masonry arch bridges. In: Proceedings of the 5th international conference on arch bridges ARCH'07. 2007. p. 515–23.
[14] Yew-Chaye Loo. Collapse load analysis of masonry arch bridges. In: Proc. 1st intl. conf. on arch bridges. Bolton; 1995. 1995.
[15] Cavicchi A, Gambarotta L. Load carrying capacity of masonry bridges: numerical evaluation of the influence of fill and spandrels. In: Proceedings of the 5th international conference on arch bridges ARCH'07. 2007. p. 609–16.
[16] Bicanic N, Ponniah D, Robinson J. Discontinuous deformation analysis of masonry bridges. In: Computational modelling of masonry, brickwork and blockwork structures. Saxe-Coburg Publications; 2001. [Chapter 7].
[17] Lemos JV. Discrete element modelling of the seismic behaviour of stone masonry arches. In: Pande GN, Middleton J, Kralj B, editors. Computer methods in structural masonry — 4. London: E & FN Spon; 1998. p. 220–7.
[18] Smars P. Etudes sur la stabilite' des arcs et voutes. Ph.D. thesis. Department of Civil Engineering, Katholieke Universiteit Leuven; 2000.
[19] Ochsendorf J. The masonry arch on spreading supports. Struct Eng 2006;17: 29–35.
[20] Ochsendorf J, Block P. Designing unreinforced masonry. In: Allen E, Zalewski W, editors. Form and forces: designing efficient, expressive structures. John Wiley and Sons; 2009. p. 215–46. [Chapter 8].
[21] Ochsendorf JA. Collapse of masonry structures. Ph.D. thesis. Cambridge: Department of Engineering, Cambridge University; 2002.
[22] Block P, DeJong M, Ochsendorf J. As hangs the flexible line: equilibrium of masonry arches. Nexus Netw J 2006;8(2):13–24.
[23] Huerta S. Mechanics of masonry vaults: the equilibrium approach. In: Proc. structural analysis of historical constructions. Guimarães; 2001.
[24] Heyman J. On shell solutions of masonry domes. Int J Solids Struct 1967;3: 177–88.
[25] Heyman J. The stone skeleton — structural engineering of masonry architecture. Cambridge: Cambridge University Press; 1995.
[26] Gago A. Análise Estrutural de Arcos, Abóbadas e Cúpulas — Contributo para o estudo do património construído. Ph.D. thesis. Lisbon: Faculty of engineering, IST-UTL tecnhical University of Lisbon; 2004 (available from www.civil.ist.utl.pt/~gago/Artigos/tese_PhD_ASGago.pdf) [in Portuguese].
[27] Crisfield MA. Finite element and mechanism methods for the analysis of masonry brickwork arches. Res. rep. 19, Crowthorne (Berks): Transport and Road Research Laboratory; 1985.

[28] Gilbert M. Limit analysis applied to masonry arch bridges: state-of-the-art and recent developments. In: Proceedings of the 5th international conference on arch bridges ARCH'07. 2007. p. 13–28.
[29] Gilbert M, Nguyen DP, Smith CC. Computational limit analysis of soil-arch interaction in masonry arch bridges. In: Proceedings of the 5th international conference on arch bridges ARCH'07. 2007. p. 633–40.
[30] Melbourne C, Gilbert M. Modelling masonry arch bridges. In: Computational modelling of masonry, brickwork and blockwork structures. Saxe-Coburg Publications; 2001. [Chapter 8].
[31] Oliveira DV, Maruccio C, Lourenço PB. Numerical modelling of a load test on a masonry arch bridge. In: Proceedings of the 5th international conference on arch bridges ARCH'07. 2007. p. 577–84.
[32] Hendry AW, Davies SR, Royles R, Ponniah DA, Forde MC, Komeyli–Birjandi F. Test on masonry arch bridge at Bargower. Contract. report 26. Crowthorne: Transport and Road Research Laboratory; 1986.
[33] Page J. Load tests to collapse on masonry arch bridges. In: Melbourne C, editor. Arch bridges: proceedings of the first international conference on arch bridges. London: Thomas Telford; 1995. p. 289–98.
[34] Gago AS, Alfaiate J, Gallardo A. Numerical analyses of the Bargower arch bridge. In: Hendriks, Rots, editors. Finite elements in civil engineering applications. Lisse (Tokyo): Swets & Zeitlinger; 2002.
[35] Harvey WJ, Maunder EAW, Ramsay ACA. The influence of spandrel wall construction on arch bridge behaviour. In: Proceedings of the 5th international conference on arch bridges ARCH'07. 2007. p. 601–8.
[36] Rots JG, Belletti B, Invernizzi S. Robust modeling of RC structures with an event-by-event strategy. Engng Fract Mech 2008;75:590–614.
[37] Alfaiate J, Gago AS, Almeida JR. On the numerical analysis of localized damage in masonry structures. In: Franco Bontempi (editor). Proceedings of the second international conference on structural and construction engineering, system-based vision for strategic and creative design. Rome; 2003. p. 769–74.
[38] Matthew JDeJong, Hendriks MAN, Rots JG. Sequentially linear analysis of fracture under non-proportional loading. Engng Fract Mech 2008;75:9042–56.
[39] Rots JG. Structural masonry. In: An experimental/numerical basis for practical design rules. Rotterdam: A.A. Balkema; 1997.
[40] Lourenço PB. Analysis of historical constructions: from thrust-lines to advanced simulations. Historical Constructions. Guimarães; 2001. p. 91–116.